Fabrication of nanostructured Ti thin film with Ti deposition in He plasmas

Kazuya Miyaguchi[1]*, Shin Kajita[2], Hirohiko Tanaka[1] and Noriyasu Ohno[1]

[1] *Graduate School of Engineering, Nagoya University, Furo-cho, Chikusa-ku, Nagoya 464-8603, Japan*

[2] *IMaSS, Nagoya University, Nagoya 464-8603, Japan*

E-mail: miyaguchi.kazuya@d.mbox.nagoya-u.ac.jp

Titanium and helium were simultaneously deposited on a titanium thin film sample to prepare a sample with nanocone structures. It was confirmed that the shape and size of the surface structure varied with the change of the amount of titanium deposition. A significant decrease in the optical reflectance was observed by the surface morphology change, and the crystal structure after oxidation treatment had an anatase structure. Combination of the anatase structure, the increase in surface area, and the decrease in reflectance could be beneficial for photocatalytic applications.

Titanium (Ti)-containing materials are used in various fields such as photocatalysts[1-5], medical applications[6, 7], structural materials for nuclear fusion[8, 9] and in semiconductor devices[10]. In the field of photocatalysis, titanium dioxide has been studied for many years for its excellent photocatalytic activity, chemical stability, and non-toxic to human body. To improve the activity of photocatalysts, extensive researches have been conducted to increase the reactive surface area at the interface with the reactants.[2-5]

In the last decade, it has been found that the surface of metals (tungsten [11], titanium[12], niobium [13], molybdenum [14], tantalum, and iron [15]) irradiated by helium (He) plasma can form nanostructures in the shape of fibers and cones. Since this structural change leads to an increase in surface area[16] and an increase in optical absorbance[17], it is expected that this method is to be applied to fabricate highly active photocatalysis.

Formation of nanostructures on titanium bulk materials have been confirmed by helium plasma irradiation, and their photocatalytic activity to decompose ethylene has also been investigated.[3, 4] The highest photocatalytic activity was observed when titanium was deposited on nanostructured tungsten. However, it was difficult to evaluate the activity of titanium alone, because the substrate tungsten was mixed with titanium. Although one of the solutions to investigate the activity of titanium alone is a usage of the bulk material, there are following issues. One is the difficulty in controlling the oxidation-layer thickness, which has a significant impact on the performance of the catalytic reaction when the catalyst is used as an electrode. Although it is known that there is an optimal thickness of oxidized layer for photocatalytic activity[18], it is not easy control the thickness of oxidized layer in a precise manner when using bulk material. Another one is a difficulty in controlling the crystal structure of titanium dioxide, because bulk materials can easily form a rutile structure after oxidation treatment. Generally, titanium dioxide has two types of structures, i.e. anatase and rutile, and it is known that samples with anatase structure show a higher activity.[19]

In this study, to address these issues, we performed helium plasma irradiation to titanium thin film. As shown later, sufficient nanostructure formation did not occur on titanium thin film samples. It was likely that this was due to a significant effect of sputtering from the substrate and not enough titanium was deposited to form the nanostructure. Therefore, we conducted helium plasma irradiation with auxiliary deposition of titanium. Recent auxiliary deposition of tungsten/rhenium have shown that this method can be a faster route to fabricate nanostructured surfaces by helium plasma treatment.[20,21] It is shown that auxiliary deposition leads to formation of nanostructured titanium thin films. From the Raman spectroscopy analysis, we also show that the fabricated thin film has anatase structure even

after oxidation.

A small-scale material irradiation device, Compact Nagoya University DIvertor Simulator (Co-NAGDIS)[22-24], was used in the experiment. The helium plasma can be generated in steady state by direct current discharge. The electron density of the plasma was $n_e \sim 2 \times 10^{18}$ m^{-3} and the electron temperature was $T_e \sim 5$ eV. Because the plasma potential was almost 0 V in this system, the applied bias corresponds to the incident ion energy. A quartz glass (10 × 10 × 0.5 mm) was used as a substrate. A negative bias against ground was applied to the substrate to control the ion energy incident to the substrate. The sample stage equipped a cooling system to maintain a constant temperature. A titanium sputtering wire (φ:1 mm, circular shape) was inserted at a distance of 10 mm from the sample stage, and titanium wire was negatively biased against ground so that the titanium atoms were sputtered out from the wire and deposited to the substrate. Separate power supplies are used for the substrate and sputtering wire, and different voltages can be applied. In this device, the plasma source, sputtering wire and substrate are located on a straight line in that order. Therefore, the helium ions in the plasma and the titanium atoms sputtered from the wire enter the substrate at the same time. The amount of deposited titanium was controlled by changing the bias applied to the sputtering wire, V_{wire}. In order to fabricate the samples, a 200 nm titanium thin film was first deposited on the quartz glass substrate in helium plasma at the substrate temperature of 550 K or less. The gas pressure was 3 Pa, V_{wire} was -165 V, and the thin film was formed with the plasma exposure time of 30 minutes. At this point, the sample surface was smooth and had a metallic color. After that, the discharge current and gas pressure were adjusted to conduct helium plasma irradiation under the following condition: the incident ion energy to the substrate was always 85 eV, the surface temperature ~ 850 K, and the helium fluence > 6×10^{25} m^{-2}. The relation between the morphology changes and the irradiation condition was previously revealed, and we tried to form spongy structure, which is a mixture of various shapes of nanostructures.[12] In this study, as we changed the amount of titanium deposition, morphology changes were examined by a scanning electron microscope (SEM: Hitachi, S4300). The changes in reflectance were measured using a UV-vis spectrophotometer (Shimadzu, UV-2600). The detector was equipped in a small integrating sphere, so that the reflectance includes both of specular and diffuse reflectance. The crystal structure of the sample was analyzed by Raman spectroscopy (Jasco, NRS-1000) using the excitation wavelength of 532 nm.

In order to quantitatively evaluate the amount of titanium ejection from the sputtering wire, the emission spectra were measured as changing V_{wire}. Fig. 1(a) shows the emission spectrum

when V_{wire} was -100 V. The measured spectrum includes both He I (388.8 nm, 447.1 nm, 471.3 nm, 492.1 nm, and 501.5 nm) and Ti (382.8 nm, 399.8 nm, and 453.3 nm) line emissions.[25] The intensities of the He I line emissions were almost the same as those at -30 V, -38 V, -60 V, and -100 V, while the intensity of the Ti I, which should be proportional to the amount of sputtered titanium atoms, increased with decreasing biasing voltage. Fig. 1(b) shows a comparison of the relationship between the sputtering yield calculated using the ACAT code [26] and the Ti I intensity at 453.3 nm (red box in Fig. 1(a)). The calculated sputtering yield of titanium wires by helium ions increased from 30 to 100 eV by more than two orders of magnitude, while Ti I increased by an order of magnitude. Although this reason was not fully understood, it might be attributable to the sputtering due to a small amount of impurity inside the device.

It is important whether the released titanium atoms from the sputtering wire are ionized before the deposition on the substrate. This is because the titanium atoms promote thin film deposition, while the titanium ions are accelerated by the bias applied to the substrate, which promotes sputtering. The ionization mean free path can be written as[27]

$$\lambda_e = \frac{v_{\mathrm{Ti}}}{n_{\mathrm{e}}<\sigma_{\mathrm{ion}} v_{\mathrm{e}}>} \qquad (1)$$

where v_{Ti} [m/s] is the speed of the sputtered Ti atom, σ_{ion} [m^2] is the ionization cross section of electrons and titanium atoms, and v_e [m/s] is the speed of the electrons. Using Eckstein, Wolfgang's data[28], we obtained v_{Ti} ~ 6 km/s for E_0 = 100 eV. Then, $<\sigma_{ion} v_e>$ is calculated to be ~8.6×10^{-14} m^3/s using σ_{ion} [m^2] in Ref [29]. By substituting the typical electron density of $n_e = 2 \times 10^{18}$ m^{-3} into Eq. (1), the mean free path is calculated to be λ_e ~ 35 mm. Because the distance between the sputtering wire and the substrate is 10 mm, roughly fourth of the ejected titanium atoms are ionized before reaching the substrate. When the above calculation was carried out from 30 eV to 165 eV, the fraction of the ionized atoms varied from 57 to 20%, suggesting that a certain amount of titanium is ionized before reaching the substrate.

Fig. 2 shows SEM micrographs on the substrate at different V_{wire}, i.e. different Ti deposition rate. Here, the incident ion energy to the substrate is always 85eV. Fig. 2(a) shows the case without the auxiliary deposition. Although the plasma exposure under the same condition have led to the formation of spongy nanostructures on bulk titanium sample[3, 4, 12], such nanostructures were not formed on the 200 nm thick thin film sample. A rough surface that was likely formed by peeling off from the substrate was identified. On W thin film samples, it was found that morphology changes by helium plasma irradiation altered from that on bulk tungsten when the thickness of the thin film was 100 nm.[30] Similar thin film effect was

likely demonstrated on the Ti thin film sample shown in Fig. 2(a). It is noted that the thickness of the thin film could be significantly thinner than original thickness of 200 nm during the helium plasma irradiation, because the sputtering was not negligible.

Fig. 2(b)-(f) show the cases when V_{wire} was -30, -38, -67, -100, and -165 V, respectively. From the top view, network of titanium nanostructures is observed in Fig. 2(b-d), and the size increases from tens of nm to sub-micrometer with decreasing the biasing voltage. The diameter of the structures was smaller than that on the bulk titanium.[4, 12)] When viewed from 45 degrees, cone-shaped structures are identified, and the size increases from sub-micrometer to several μm with increasing the amount of deposition. The size of the cone was almost consistent with those formed on bulk titanium.[12)] When V_{wire} was -100 V, no mesh-like structure can be seen on the surface; it is found that cone structures are clustered together and have grown to about 5 μm. At V_{wire} of -165 V, the sample has an uneven surface structure and the nanocone structure has disappeared.

It is interesting to note that the height of the cone structures in Fig. 2(d,e) is comparable or larger than several μm, which is much greater than the original thickness of the thin film deposited on the substrate (200 nm). Thus, the results suggested that the nanocones were not formed by the sputtering of the thin film, but the deposited titanium atoms/ions played a significant role for the nanocone formation. Also, the increase in the size of nanocones from V_{wire} of -30 to -100 V also supported the role of deposited titanium. It is known that the sputtering has contributed to the formation of nanocones during the helium plasma irradiation.[31)] However, it is not clear now how the auxiliary titanium deposition contributed to the enhancement of the formation of nanocones on thin films. One potential mechanism is the combination of the formation of thin layer by titanium atoms and accelerated sputtering by titanium ions. As was discussed earlier, more than 40-80% of the released titanium atoms will reach the sample without ionization. The deposited atoms should contribute to the formation of thin layer during the helium plasma irradiation. At the same time, ionized titanium contributed to the formation of nanocones with a higher sputtering yield. When decreasing V_{wire}, since the speed of the released titanium atoms increases, the fraction of the ionization decreases. The disappearance of nanocones at V_{wire} of -165 V might be caused by the increase in the deposition of titanium atoms.

Fig. 3 shows the wavelength dependence of optical reflectance. In addition to the samples shown in Fig. 2, a thin film sample without additional helium plasma irradiation (smooth thin film) is also shown for comparison. On the smooth thin film sample, the reflectance was in the range of 40-60%. With the auxiliary deposition, the reflectance was less than that on

the smooth thin film sample; it was less than 10% at the wavelength range of <700 nm when V_{wire} was from -30 to -100 V. The results revealed that the optical reflectance decreased by the formation of nanostructures similar to bulk titanium cases.[17] When V_{wire} was -165 V, the reflectance was in the range of 20-40%, which was higher than those with higher V_{wire}. This was because the surface became flatter than those at higher V_{wire}.

The nanostructured sample at V_{wire} of -30V (called Ti_{nano} hereafter) and the smooth thin film sample without additional helium plasma irradiation (called Ti_{stf} hereafter) were oxidized at oxidation temperatures, T_o, of 773, 873, and 973 K for 30 min. Fig. 4(a) and (b) shows and Raman spectrum of Ti_{nano} and Ti_{stf}, respectively, oxidized at different temperatures. The peaks of the rutile and anatase structures[32] are shown as R and A, respectively in Fig. 4(a) and (b). Fig. 4(a) shows that the anatase structure remains even when treated at 973 K, while on Ti_{stf}, anatase structure is gradually changed to rutile structure as the oxidation temperature is increased. It is known that the transition of the anatase to the rutile occurs at a certain transition temperature, which is varied by processing method.[33] The results suggested that the helium plasma irradiation with auxiliary deposition increased the transition temperature.

It has also been confirmed that the titanium bulk sample has mainly a rutile structure when oxidized at 773K.[3] On the other hand, on Ti_{stf}, anatase structure was identified even at 873 K, indicating that the transition temperature increased on the thin film formed in helium plasma environment even without additional helium plasma irradiation with auxiliary deposition. Previously, it was shown that thin film formed using a magnetron sputtering apparatus on a tungsten substrate under an argon atmosphere only has rutile structures at the oxidization temperature of 773 K.[4] Thus, the conditions in the present study includes a factor to increase the transition temperature from rutile to anatase. There are two possible causes: formation of thin film in a helium atmosphere and a higher substrate temperature during the deposition. The increase in the transition temperature was probably because the crystallinity of the nanostructured samples was more disordered than that of the smooth ones. Helium bubble growth should have been accelerated in helium plasma environment at higher substrate temperature. Considering the position of the bandgap, it is suggested that a mixture of rutile and anatase structures may enhance the separation of the electron-hole pairs generated by light irradiation due to the difference in the bandgap.[34] Therefore, it is of interest to investigate the photocatalytic performance as changing the oxidization temperature for the samples fabricated in this study.

In summary, when the helium plasma was irradiated at the incident ion energy to the

substrate of~ 85 eV, the surface temperature of ~ 850 K, and the helium fluence (~8.0×10^{25} m^{-2}) with auxiliary titanium deposition, nanostructures with nanocones were formed on the surface, and the morphology change depended on the amount of titanium deposition. From the measurement of the optical reflectance of the samples with nanostructured surfaces, it was found that the optical reflectance decreased by the morphology change. Furthermore, the crystal structure was identified after the oxidation treatment using Raman spectroscopy. The transition temperature from rutile to anatase was higher than that of bulk titanium or titanium thin film samples formed in magnetron sputtering device with argon atmosphere, suggesting that the crystal structure could be controlled by using thin film samples fabricated in this study. It is expected that the method used in this study will fabricate a high photocatalytic activity with a high surface area, low optical absorbance, and a controlled crystal structure. In the future work, we plan to investigate the photocatalytic activity using the sample fabricated in this work.

Acknowledgments

This work was supported in part by a Grant-in-Aid for Scientific Research 17KK0132, 19H01874 from the Japan Society for the Promotion of Science (JSPS), and the NIFS Collaboration Research program (NIFS19KOAH036).

References

1) A. Fujishima, and K. Honda, Nature **238**(5358), 37-38 (1972).
2) M. L. V. de Chiara, S. Pal, A. Licciulli, M. L. Amodio, and G. I. A. N. C. A. R. L. O. Colelli, Biosystems Engineering **132**, 61-70 (2015).
3) S. Kajita, Y. Tomita, E. Yasunaga, T. Yoshida, K. Miyaguchi, H. Tanaka, and N. Ohno, Jpn. J. Appl. Phys. **58**(7), 070903 (2019).
4) Y. Tomita, S. Kajita, E. Yasunaga, T. Yoshida, N. Ohno, and H. Tanaka, Jpn. J. Appl. Phys. **58**(SE), SEEG01 (2019).
5) S. Shen, J. Chen, M. Wang, X. Sheng, X. Chen, X. Feng, and S. S. Mao, Prog. Mater. Sci. **98**, 299-385 (2018).
6) M. Kulkarni, A. Mazare, E. Gongadze, Š. Perutkova, V. Kralj-Iglič, I. Milošev, P. Schmuki, and M. Mozetič, Nanotechnology **26**(6), 062002 (2015).
7) N. A. Riedel, Plasma processing for nanostructured topographies (Doctoral dissertation, Colorado State University) (2012).
8) P. Marmy, T. Leguey, I. Belianov, and M. Victoria, J. Nucl. Mater. **283**, 602-606 (2000).
9) Raul. dos Santos, J. Nucl. Mater. **155**, 589-591 (1988)
10) L. Gao, J. Gstöttner, R. Emling, M. Balden, C. Linsmeier, A. Wiltner, W. Hansch, and D. Schmitt-Landsiedel, Microelectron Eng. **76**(1-4), 76-81 (2004).
11) S. Takamura, N. Ohno, D. Nishijima, and S. Kajita, Plasma Fusion Res. **1**, 051-051 (2006).
12) S. Kajita, D. Kitaoka, N. Ohno, R. Yoshihara, N. Yoshida, and T. Yoshida, Appl. Surf. Sci. **303**, 438-445 (2014).
13) S. Kajita, F. Mimuro, T. Yoshida, N. Ohno, and N. Yoshida, Chemphyschem **19**(23), 3237-3246 (2018).
14) S. Takamura, Plasma Fusion Res. **9**, 1405131-1405131 (2014)
15) S. Kajita, T. Ishida, N. Ohno, D. Hwangbo, and T. Yoshida, Sci. Rep. **6**(1), 1-10 (2016).
16) M. Yajima, Y. Hatano, S. Kajita, J. Shi, M. Hara, and N. Ohno, J. Nucl. Mater. **438**, S1142-S1145 (2013).
17) S. Kajita, T. Yoshida, D. Kitaoka, R. Etoh, M. Yajima, N. Ohno, H. Yoshida, N. Yoshida, and Y. Terao, J. Appl. Phys. **113**(13), 134301 (2013).
18) J. H. Kennedy, and K. W. Frese Jr., J. Electrochem. Soc. **125.5,** 723 (1978).
19) K. Tanaka, M. F. Capule, and T. Hisanaga, Chem. Phys. Lett. **187**(1-2), 73-76 (1991).
20) S. Kajita, S. Kawaguchi, N. Ohno, and N. Yoshida, Sci. Rep. **8**(1), 1-9 (2018).

21) S. Kajita, T. Nojima, T. Okuyama, Y. Yamamoto, N. Yoshida, and N. Ohno, Acta Mater. **181**, 342-351 (2019).

22) K. Asai, N. Yoshida, N. Ohno, S. Kajita, H. Tanaka, M. Yajima, and D. Nagata, Plasma Fusion Res. **15**, 1201004-1201004 (2020).

23) Q. Shi, S. Kajita, N. Ohno, M. Tokitani, D. Nagata, and S. Feng, J. Appl. Phys. **128**(2), 023301 (2020).

24) S. Kajita, K. Asai, N. Ohno, H. Tanaka, N. Yoshida, D. Nagata, and M. Yajima, J. Nucl. Mater. 152350 (2020).

25) NIST database https://www.nist.gov/pml/atomic-spectra-database

26) Y. Yamamura, and Y. Mizuno, Inst. Plasma Physics, Nagoya Univ., IIPJ-AM-40 (1985).

27) R. J. Goldston, and P. H. Rutherford, *Introduction to Plasma Physics* (Routledge, New York,1995), p155

28) Eckstein, and Wolfgang. "Calculated sputtering, reflection and range values." (2002).

29) A. V. Philippov, V. M. Povyshev, A. A. Sadovoy, V. P. Shevelko, G. D. Shirkov, E. G. Vasina, and V. V. Vatulin, JINR Commun. (2002).

30) S. Feng, S. Kajita, Y. Tomita, T. Yoshida, and N. Ohno, Jpn. J. Appl. Phys. **59**(SA), SAAB04 (2019).

31) D. Nishijima et al., Nucl. Mater. Energy **18**, 67-71 (2019).

32) B. Henkel, T. Neubert, S. Zabel, C. Lamprecht, C. Selhuber-Unkel, K. Rätzke, T. Strunskus, M. Vergöhl, and F. Faupel, Appl. Catal. B **180**, 362-371 (2016).

33) D. A. Hanaor, and C. C. Sorrell, J. Mater. Sci. **46**(4), 855-874 (2011).

34) D. O. Scanlon et al., Nature materials **12**(9), 798-801 (2013).

Figure Captions

Fig. 1. (a) Emission spectrum (V_{wire} = -100 V) and (b) the incident ion energy dependences of the Ti I intensity and calculated sputtering yield.

Fig. 2. SEM micrographs on titanium surfaces at different V_{wire}: (a) w/o the sputtering wire, (b) -30 V, (c) -38 V, (d) -67 V, (e) - 100V, and (f) -165 V.

Fig. 3. Optical reflectance of a smooth titanium film sample (dashed line) and samples formed at different V_{wire} (-30, -38, -67, -100, and -165 V).

Fig. 4. (a) Raman spectra of a nanostructured sample prepared with a sputtering wire at V_{wire} of -30 V and (b) a smooth sample prepared at a substrate temperature of 550 K.

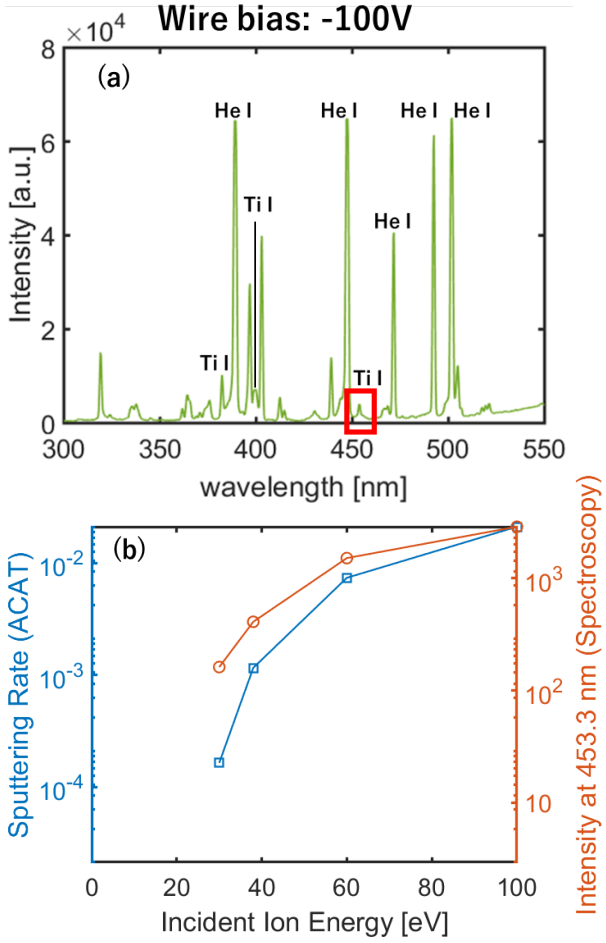

Fig.1.

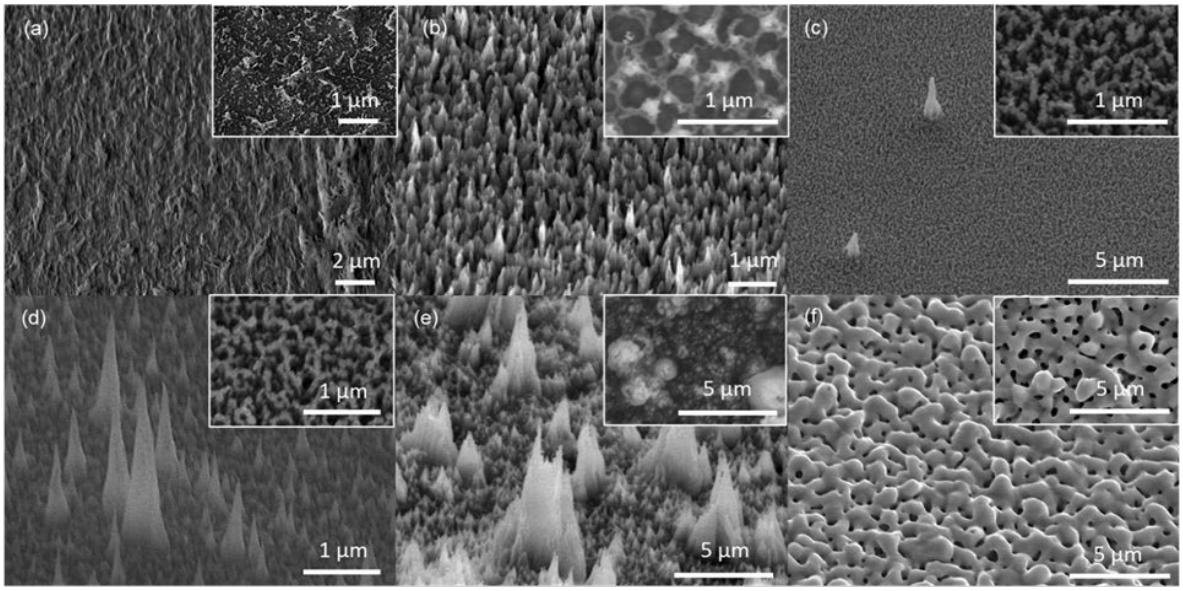
(a)
1 μm
2 μm
(b)
1 μm
1 μm
(c)
1 μm
5 μm
(d)
1 μm
1 μm
(e)
5 μm
5 μm
(f)
5 μm
5 μm

Fig. 2.

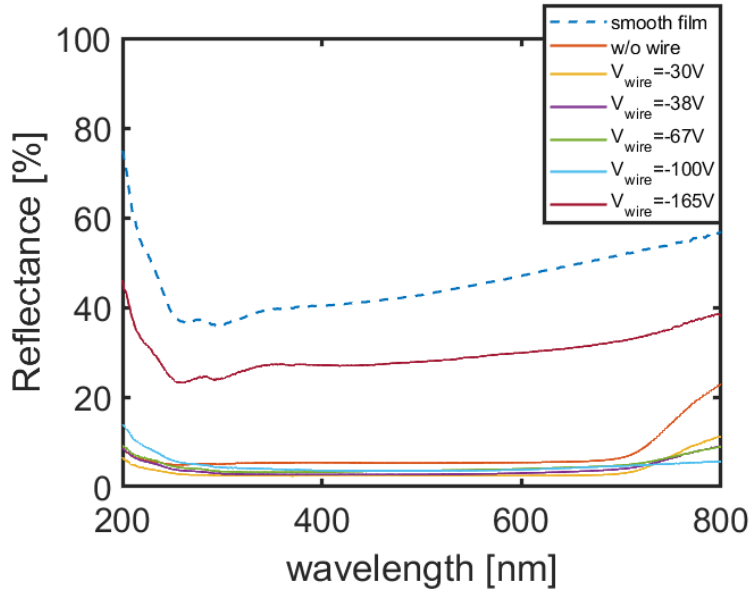
smooth film
w/o wire
V wire =-30V
V wire =-38V
V wire =-67V
V wire =-100V
V wire =-165V
Reflectance [%]
100
80
60
40
20
0
200
400
600
800
wavelength [nm]

Fig. 3.

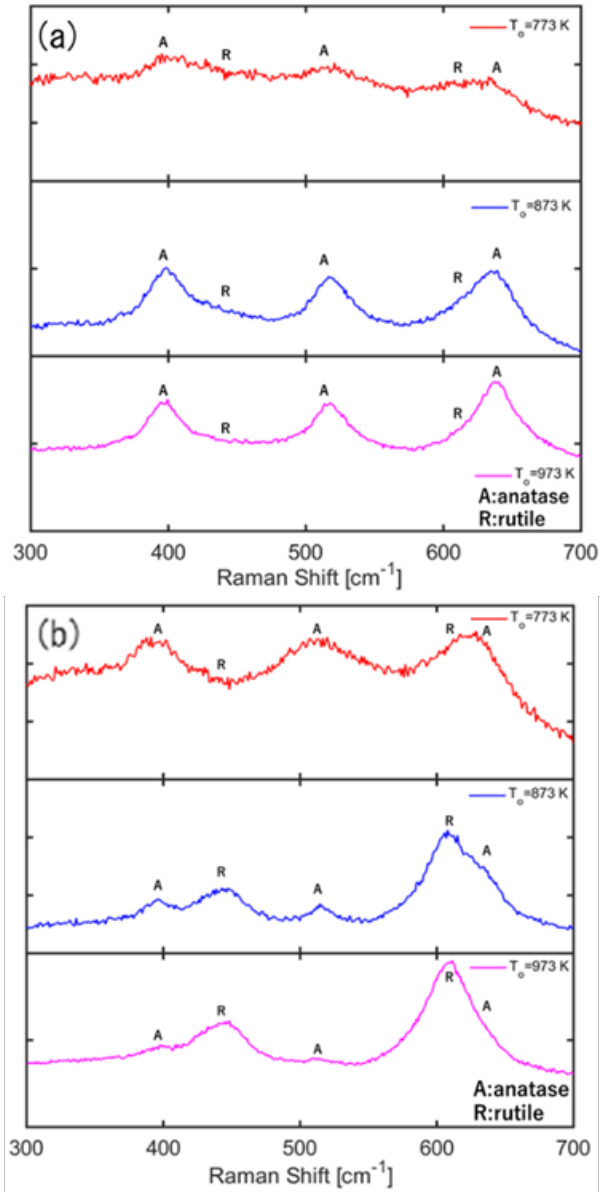
(a)
T_o=773 K
T_o=873 K
T_o=973 K
A:anatase
R:rutile
300
400
500
600
700
Raman Shift [cm^-1]
(b)
T_o=773 K
T_o=873 K
T_o=973 K
A:anatase
R:rutile
300
400
500
600
700
Raman Shift [cm^-1]

Fig. 4.